

# Molecular Order and Density of Skin and Core in Drawn Polypropylene Investigated by Spectroscopic $^{13}\text{C}$ NMR Imaging

E. Günther, B. Blümich, and H. W. Spiess\*

Max-Planck-Institut für Polymerforschung, Postfach 3148,  
D-6500 Mainz, Federal Republic of Germany

Received September 16, 1991

**Introduction.** Molecular order and the ratio between crystalline and amorphous portions are important factors determining the macroscopic properties of polymeric materials.<sup>1</sup> Spatial variations of the molecular parameters, depending on the processing conditions, lead to nonuniform and spatial-dependent macroscopic behavior. For a systematic improvement of the manufacturing process, methods which record the spatial dependence of order and crystallinity are in need. On a phantom of deuterated polyethylene we have recently shown that solid-state  $^2\text{H}$  NMR spectroscopy, in combination with magnetic-field gradients for spatial encoding, can indeed provide the desired information for bulk samples.<sup>2</sup> It is the purpose of this paper to demonstrate that spectroscopic images with  $^{13}\text{C}$  in natural abundance can be recorded for a "real" polymer material, where spatial heterogeneities are known to exist.

In injection-molded polypropylene a spatially heterogeneous structure of skin and core is observed with a polarizing microscope. The thickness of the skin layer is, depending on the kind of resin and molding conditions, between 100 and 600  $\mu\text{m}$ . The different structures have been studied by X-ray methods, electron microscopy, DSC, and mechanical techniques. It was found that the skin and core layers possess different melting behaviors and mechanical properties due to differences in molecular ordering, orientation, and morphology.<sup>3</sup>

On samples that are stationary in the magnetic field one can determine molecular order and dynamics by analyzing the NMR line shape. Signals from amorphous and crystalline parts can be separated by different pulse techniques.<sup>4</sup> Spatial encoding of the NMR signal is accomplished via magnetic-field gradients, which so far have been mainly employed for proton NMR imaging of biological tissues<sup>5</sup> and for investigations of elastomer materials.<sup>6</sup>

**Experimental Section and Results.** By means of a modified two-dimensional (2D) NMR method<sup>7</sup> (the pulse sequence is given in Figure 1), it is possible to record for each point in space, the corresponding  $^{13}\text{C}$  NMR spectrum. In this way, molecular order and crystallinity are spatially encoded for a given portion of the sample, thereby allowing direct correlation of spectral and spatial information. The NMR imaging experiments were performed on a Bruker MSL-300 spectrometer ( $^{13}\text{C}$  Larmor frequency 75.47 MHz) with a commercial double-resonance probe that has been equipped with a gradient system and a low-pass filter to prevent interference between the gradient driver and the radio frequency (rf) circuit. The gradient system is capable of delivering magnetic-field gradients of 36 G/cm with 30- $\mu\text{s}$  switching times in three orthogonal directions.

An injection-molded sample of syndiotactic polypropylene (sPP) with the geometry displayed in Figure 2 has been investigated. The sPP sample ( $M_w \approx 150\text{K}$ ) was drawn to 500% and retained a final elongation of approximately 300% after loosening the grips.<sup>8</sup> One-dimensional spatial resolution along the  $x$ -axis (cf. Figure

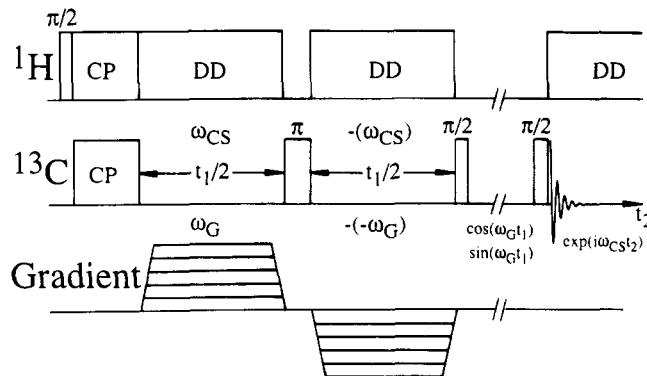


**Figure 1.** Pulse sequence for spectroscopic  $^{13}\text{C}$  NMR imaging. The chemical shift is refocused by the  $\pi$  pulse, the gradient reversed to preserve spatial encoding. In a Fourier imaging scheme a two-dimensional data set is recorded by stepping the gradient strength.

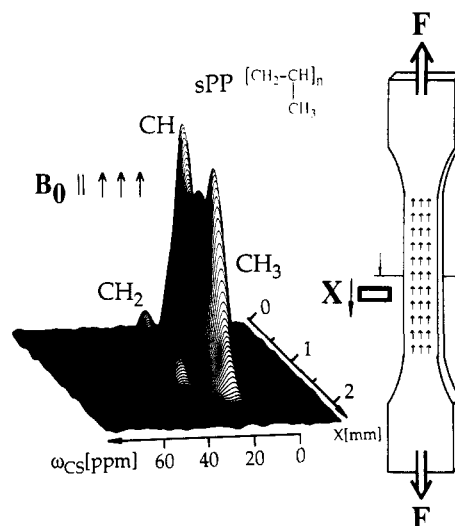


**Figure 2.** Geometry of the sample and stacked plot of the CP image recorded with the draw axis parallel to the static magnetic field.

2) is sufficient for definite spatial encoding, because the skin layers along the short sides of the sample were removed.

For the sPP sample four images have been recorded: two where the carbon magnetization was created by 1-ms cross polarization (CP) from protons and two without CP where the carbon magnetization was created by spin-lattice relaxation (one-pulse excitation). With CP the signals of the crystalline regions are recorded for all three carbon atoms in the monomer unit, whereas for one-pulse excitation only the methyl carbons contribute due to their short spin-lattice relaxation time  $T_1$ . The  $\pi/2$  pulse length was 2.5  $\mu\text{s}$ , the repetition time was 2 s for the CP and 2 s for the non-CP experiments, and each 2D spectrum took 22 h to acquire. Two images have been recorded with each technique. For one image, the sample was positioned so that the static magnetic field  $B_0$  was parallel to the draw axis, whereas for the other image it was perpendicular to it.

From the images shown in Figures 2 and 3, three effects are observed.

(1) The density of the skin layer is higher than that of the core: The density effect can be judged clearly from the lower spectral intensity in the core layer, especially for the spectrum of the methine carbon which is relatively insensitive to orientation effects due to its small chemical shift anisotropy (cf. Figure 2). Contour plots of all images

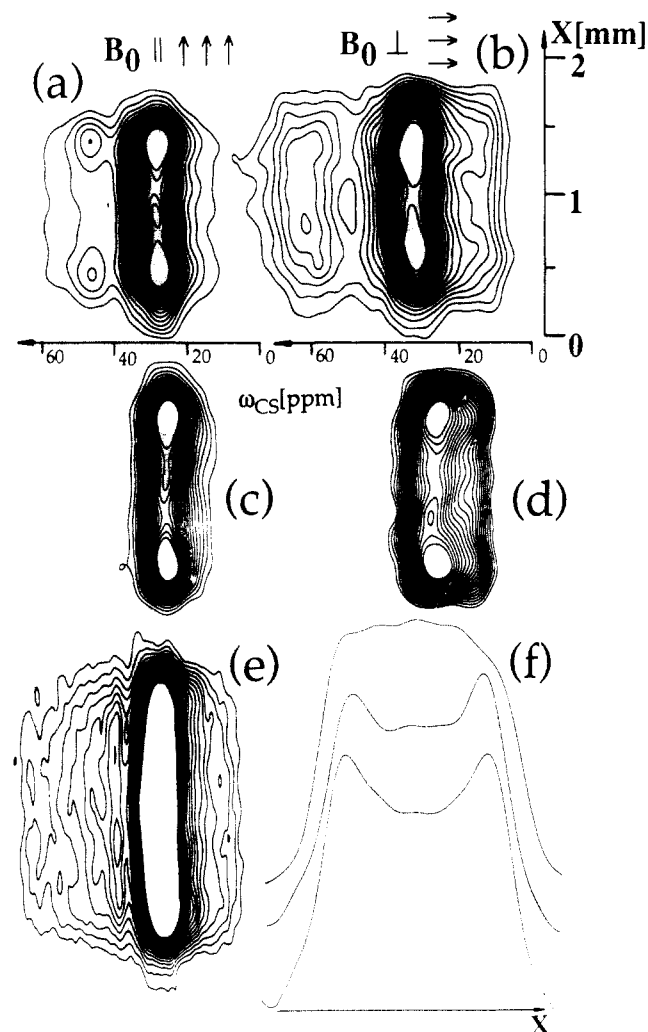


**Figure 3.** Contour plots of all recorded  $^{13}\text{C}$  NMR images. CP images with the draw axis (a) parallel and (b) perpendicular to the static magnetic field. (c and d) same as in a and b but with one-pulse excitation. Note the different positions of the maximal intensity (white spots), comparing CP spectra with the dominating methine signal and non-CP spectra where only the methyl carbons contribute. (e) CP image of unoriented and homogeneous sPP. Projections onto the spatial axis for the unoriented and homogeneous sPP (top) and drawn sPP recorded with CP (middle) and without CP (bottom).

are collected in Figure 3. Comparison of the CP images in Figure 3a,b with the images in Figure 3c,d recorded using one-pulse excitation establishes that the lower spectral intensity of the core layer is caused by lower material density and not by variations of the CP efficiency arising from changes in the ratio between crystalline and amorphous regions. The intensity variation cannot result from  $B_1$  inhomogeneity, because the sample fills less than 20% of the solenoid (12 mm in length). Analyzing the spin density represented by projections onto the spatial axis in Figure 3f shows that the density of the 350- $\mu\text{m}$ -thick skin layer is  $22 \pm 3\%$  higher than that of the 1000- $\mu\text{m}$ -thick core. The density variation has also been verified quantitatively by flotation, using pieces from the core and the skin, respectively.

(2) The chains in both layers are oriented parallel to the draw axis: The chain orientation becomes apparent by

comparison of the images recorded with different orientations between  $B_0$  and the draw axis. In both cases, with CP and without CP, the spectral intensity is concentrated between 20 and 50 ppm (all values relative to tetramethylsilane) for the parallel orientation (cf. Figure 3a) because the frequency is determined only by the width of the orientational distribution. For the perpendicular orientation however, it is necessary to account for an additional planar distribution that creates frequency components over the whole chemical anisotropy range, from 6 to 70 ppm (cf. Figure 3b), and results in a lower signal-to-noise ratio. In addition to the chemical shift principal values of isotactic polypropylene,<sup>9</sup> for sPP the  $\gamma$ -gauche effect leads to two 8.7 ppm spaced isotropic shifts<sup>10</sup> for the methylene carbon that are unresolved in the static spectrum. For comparison, an image of unoriented and homogeneous sPP is shown in Figure 3e.

(3) The chain order is slightly higher in the skin layer: From the stacked plot in Figure 2 it can easily be seen that the skin layer is characterized by a slightly higher orientation. This is best seen in the methylene signals which manifest a high chemical shift anisotropy and exhibit only small overlap with the methine and the methyl resonances. Because of the higher molecular order, the methylene carbon signals are, when corrected for the lower density in the core, still higher and narrower in the skin layer. A line-shape analysis, assuming a Gaussian distribution of orientations, suggests a full width at half-maximum height of  $30^\circ$  for the skin layer and  $40^\circ$  for the core layer.

This investigation thus clearly demonstrates that spectroscopic  $^{13}\text{C}$  NMR imaging can provide significant information on the spatial dependence of density, order, and crystallinity in heterogeneous polymeric materials.

**Acknowledgment.** We thank Dr. D. Müller and Dr. L. Wunsch, Bruker GmbH, Karlsruhe, FRG, for providing the probe and the gradient system and Hanspeter Raich for expertly designing the low-pass filter. We also express our thanks to Dr. M. Fleissner, Forschung und Entwicklung, Hoechst Aktiengesellschaft, Frankfurt/Main, FRG, for the drawn syndiotactic polypropylene sample. Financial support from the Deutsche Forschungsgemeinschaft (Leibniz program) is gratefully acknowledged.

## References and Notes

- (1) *Principles of Polymer Engineering*; McCrum, N. G., Buckley, C. P., Bucknall, C. B., Eds.; Oxford University Press: Oxford, U.K. 1988.
- (2) Günther, E.; Blümich, B.; Spiess, H. W. *Mol. Phys.* **1990**, *71*, 477.
- (3) Fujiyama, M.; Wakino, T.; Kawasaki, Y. *J. Appl. Polym. Sci.* **1988**, *35*, 29.
- (4) *High Resolution NMR Spectroscopy of Synthetic Polymers in Bulk*; Komoroski, A., Ed.; VCH: Weinheim, FRG, 1986.
- (5) *Biomedical Magnetic Resonance Imaging*; Wehrli, F. W., Shaw, D., Kneeland, J. B., Eds.; VCH: Weinheim, FRG, 1988.
- (6) Smith, S. R.; Koenig, J. L. *Macromolecules* **1991**, *24*, 3496.
- (7) Fry, C. G.; Lind, A. C.; Davis, M. F.; Duff, D. W.; Maciel, G. E. *J. Magn. Reson.* **1989**, *83*, 656.
- (8) Fleissner, M. Private communication, Hoechst AG Frankfurt/Main am Main.
- (9) Nakai, T.; Ashida, J.; Terao, T. *Magn. Reson. Chem.* **1989**, *27*, 666.
- (10) Bunn, A.; Cudby, M. E. A. *J. Chem. Soc., Chem. Commun.* **1981**, 15.